New Phytologist

Research

The auxin efflux carrier PIN1a regulates vascular patterning in cereal roots

Riccardo Fusi[1,2], Sara Giulia Milner[3], Serena Rosignoli[3], Riccardo Bovina[3], Cristovão De Jesus Vieira Teixeira[1,4], Haoyu Lou[1,5,6], Brian S. Atkinson[1], Aditi N. Borkar[7], Larry M. York[1,8], Dylan H. Jones[1], Craig J. Sturrock[1], Nils Stein[9,10], Martin Mascher[9,11], Roberto Tuberosa[3], Devin O'Connor[12], Malcolm J. Bennett[1,2], Anthony Bishopp[1], Silvio Salvi[3] and Rahul Bhosale[1,2,13]

[1]School of Biosciences, University of Nottingham, Sutton Bonington Campus, Nottingham, LE12 5RD, UK; [2]Future Food Beacon of Excellence, University of Nottingham, Sutton Bonington Campus, Nottingham, LE12 5RD, UK; [3]Department of Agricultural and Food Sciences, University of Bologna, Viale Fanin 44, 40127, Bologna, Italy; [4]Laboratory of Cell and Molecular Biology, Institute of Biology, University of Neuchâtel, Neuchâtel, Switzerland; [5]School of Agriculture, Food and Wine, Waite Research Institute, The University of Adelaide, Urrbrae, SA, 5064, Australia; [6]Australian Plant Phenomics Facility, The University of Adelaide, Waite Campus, Urrbrae, SA, 5064, Australia; [7]School of Veterinary Medicine and Science, University of Nottingham, LE12 5RD, Nottingham, UK; [8]Biosciences Division, Oak Ridge National Laboratory, Oak Ridge, TN 37830, USA; [9]Leibniz Institute of Plant Genetics and Crop Plant Research (IPK) Gatersleben, 06466, Seeland, Germany; [10]Department of Crop Sciences, Center of integrated Breeding Research (CiBreed), Georg-August-University, Von Siebold Str. 8, 37075, Göttingen, Germany; [11]German Centre for Integrative Biodiversity Research (iDiv) Halle-Jena-Leipzig, Leipzig, Germany; [12]Sainsbury Laboratory, Cambridge University, 47 Bateman Street, Cambridge, CB2 1LR, UK; [13]International Crops Research Institute for the Semi-Arid Tropics (ICRISAT), Patancheru, 502324, Telangana, India

Authors for correspondence:
Rahul Bhosale
Email: rahul.bhosale@nottingham.ac.uk

Silvio Salvi
Email: silvio.salvi@unibo.it

Received: *16 January 2024*
Accepted: *29 March 2024*

New Phytologist (2024)
doi: 10.1111/nph.19777

Key words: auxin efflux carrier, barley, PIN1, root, vascular development.

Summary

- Barley (*Hordeum vulgare*) is an important global cereal crop and a model in genetic studies. Despite advances in characterising barley genomic resources, few mutant studies have identified genes controlling root architecture and anatomy, which plays a critical role in capturing soil resources.
- Our phenotypic screening of a TILLING mutant collection identified line *TM5992* exhibiting a short-root phenotype compared with wild-type (WT) Morex background. Outcrossing *TM5992* with barley variety Proctor and subsequent SNP array-based bulk segregant analysis, fine mapped the mutation to a cM scale. Exome sequencing pinpointed a mutation in the candidate gene *HvPIN1a*, further confirming this by analysing independent mutant alleles.
- Detailed analysis of root growth and anatomy in *Hvpin1a* mutant alleles exhibited a slower growth rate, shorter apical meristem and striking vascular patterning defects compared to WT. Expression and mutant analyses of *PIN1* members in the closely related cereal brachypodium (*Brachypodium distachyon*) revealed that *BdPIN1a* and *BdPIN1b* were redundantly expressed in root vascular tissues but only *Bdpin1a* mutant allele displayed root vascular defects similar to *Hvpin1a*.
- We conclude that barley *PIN1* genes have sub-functionalised in cereals, compared to Arabidopsis (*Arabidopsis thaliana*), where *PIN1a* sequences control root vascular patterning.

Introduction

Barley is the fourth most significant cereal crop in the world, following wheat, maize and rice. This crop is increasingly utilised in genetic studies due to its diploid nature, low chromosome number, ease of cross-breeding and cultivation in different climatic conditions. In recent years, considerable progress has been made in generating novel genetic resources in barley, including a high-quality genome, gene knockout collections for reverse genetics, marker rich genetic diversity panels and synthetic recombinant populations for association genetics (Nice *et al.*, 2016; Mascher *et al.*, 2017; Schreiber *et al.*, 2019). To effectively utilise these resources in genetic improvement or crop breeding approaches, it is necessary to efficiently link genes to important agronomic traits. For instance, root traits play critical roles in water and nutrient foraging in soil. Thus, pinpointing genes underlying root function would enable the development of crop varieties with improved root systems. Although several barley mutants related to root hair, cytokinin homeostasis and root angle have been characterised (Gahoonia *et al.*, 2001; Chmielewska *et al.*, 2014; Gasparis *et al.*, 2019; Kirschner *et al.*, 2021, 2024; Fusi *et al.*, 2022), genes that regulate key root architectural and anatomical traits remain to be identified.

The plant hormone auxin plays a crucial role in plant morphogenesis, including root growth and development (Bennett *et al.*, 1996; Benková *et al.*, 2003; Reinhardt *et al.*, 2003; Petrášek *et al.*, 2006; Wiśniewska *et al.*, 2006; Swarup & Péret, 2012; Adamowski & Friml, 2015). Auxin is unique amongst plant hormones in having a specialised transport system that mobilises this signal in a polarised manner between cells and tissues (Bennett *et al.*, 1996; Wiśniewska *et al.*, 2006; Swarup & Péret, 2012). AUX1/LAX auxin influx carriers transport auxin into plant cells, while PIN efflux carriers pump auxin out of plant cells (Swarup & Bhosale, 2019). The PIN class of auxin efflux carriers are often asymmetrically localised in plant cells plasma membranes, which contributes to the polarised movement of auxin and formation of hormone gradients that regulate plant growth, positioning of organs and patterning of tissues (Petrášek *et al.*, 2006; Wiś niewska *et al.*, 2006; Adamowski & Friml, 2015). In the plant model Arabidopsis (*Arabidopsis thaliana*), PIN1 is a major auxin transporter whose functions have been described during leaf initiation, leaf margin definition and shoot vascular patterning, embryo development, root gravitropism (Benková *et al.*, 2003; Reinhardt *et al.*, 2003; Leyser, 2005; Hay *et al.*, 2006; Scarpella *et al.*, 2006; Bilsborough *et al.*, 2011; Xi *et al.*, 2016). Recent research has revealed functional diversity of *PIN1* in grasses compared to Arabidopsis and the Brassicaceae. Brachypodium (*Brachypodium distachyon*) has two PIN1 clade members *PIN1a* and *PIN1b* and a phylogenetic sister to the PIN1 clade *SoPIN1*, which collectively recapitulate expression domains and polarisation behaviours observed for AtPIN1 in Arabidopsis (O'Connor *et al.*, 2014, 2017). Similarly, barley has *PIN1a*, *PIN1b* and *SoPIN1* genes that are one-to-one orthologues of brachypodium PIN1 members (Supporting Information Fig. S1).

During shoot development in Arabidopsis, PIN1 is expressed in the epidermis and vasculature (Guenot *et al.*, 2012). During spikelet development in brachypodium, SoPIN1 is expressed in the epidermis, PIN1a in inner vasculature and PIN1b in parenchymatic tissues between epidermis and vasculature, indicating a potential role in supporting vasculature formation in the new developing organ (O'Connor *et al.*, 2014). In Arabidopsis roots, the PIN1 protein is asymmetrically localised rootwards in central stele and cortical cells, whereas it is localised shootwards in epidermal cells (Blilou *et al.*, 2005). This pattern of localisation, when combined with other PIN family members (PIN2, 3, 4, and 7), plays a crucial role maintaining the rootward/shootward auxin polarity which sustain the regular cell division and organ patterning in roots (Gälweiler *et al.*, 1998; Reinhardt *et al.*, 2003; Blilou *et al.*, 2005; Zhang *et al.*, 2019). Similarly, to Arabidopsis PIN1, HvPIN1a is localised in barley root meristem cells in a rootward direction towards the QC in the inner tissues and shootwards in outer cortex epidermis lateral root cap cells, suggesting a similar pattern of auxin fluxes in this species (Kirschner *et al.*, 2018). However, the roles of the individual cereal PIN1 clade members during root growth and development remains unclear.

Through a combination of forward genetic and genomic approaches in barley, we identified mutations in the *PIN1a* gene that cause defects in root developmental and vascular patterning. These defects were mimicked in wild-type (WT) roots by blocking PIN1-mediated polar auxin transport using the inhibitor NPA. Furthermore, expression domain and root growth analysis of reporters and mutants of *PIN1* members in the cereal model brachypodium suggested that BdPIN1a and BdPIN1b act redundantly during root vascular patterning with BdPIN1a functioning as a central regulator. We conclude by discussing the functional diversity of PIN1 in cereals and conserved role of PIN1a controlling root vascular patterning.

Materials and Methods

Plant material

Barley (*Hordeum vulgare* L.) *HvPIN1a* mutant alleles (*TM5992*, *TM5141* in cultivar cv Morex and *TB13081* in cultivar cv Barke background), brachypodium *BdPIN1* member mutants (*Bdpin1a* and *Bdpin1b* in Bd21.3 background) (O'Connor *et al.*, 2017) and respective WT (Morex, Barke and TB_WT and Bd21.3, respectively) were used for root length and cross-section imaging analyses. All barley *Hvpin1a* mutant alleles and their respective WT lines were used for root tip staining and confocal imaging. Morex was used in NPA treatment assay. Morex, TM5141 and TM5992 were used in NAA treatment assay. The brachypodium auxin response reporter DR5 and auxin efflux carrier reporters PIN1a, PIN1b, and SoPIN1 (O'Connor *et al.*, 2017) were employed for expression analysis in root tip and vasculature tissues through confocal microscopy.

Growth conditions

For all root growth and cross-section phenotyping analyses of barley, seeds were surface sterilised with 20% Sodium hypochlorite solution for 5 mins followed by five washes with sterile water. Sterilised seeds were germinated on sterile Whatman filter paper placed in a Petri dish for 1 d at 21°C in dark. Germinated barley seedlings were transferred to 1% agar plates (without MS) at pH 5.7 in growth room (21°C, 16 h : 8 h, day : night cycle; 125–150 μmol m^{-2} s^{-1}) and grown vertically up to 7 d. Brachypodium seeds were surface sterilised using the same method above and then grown in ½-strength Murashige & Skoog medium, 1% agar plates at pH 5.7 at the same environmental conditions as above for 7 d.

Identification of barley short-root mutant lines *TM5992*, *TM5141* and *TB13081*

Barley short-root mutant (*TM5992*) was identified as described in Bovina *et al.* (under preparation). Briefly a chemically (NaN_3) mutagenised population (TILLMore population) (Talamè *et al.*, 2008) of *c.* 4000 M6 lines in Morex cv background was screened for root traits at the seedling (2-wk-old) stage. *TM5992* showed a short-root phenotype when grown using semi-hydroponics method adapted from (Talamè *et al.*, 2008), when compared to Morex WT. From the same mutagenised population, a second short-root mutant line (*TM5141*) was

identified. A third *HvPIN1a* mutant allele (*TB13081*) was further identified by TILLING (McCallum *et al.*, 2000) by screening an EMS (Ethyl methanesulfonate) treated population of cv Barke consisting of 10 279 individuals, for which a multidimensional pool of individual DNA samples is available (Gottwald *et al.*, 2009). All mutations found using a capillary electrophoresis system were further validated by re-sequencing using Sanger sequencing and following primers: 5141_F1 GGACTTCTACCACGTCATGAC, 5992_F2 GGACTTC TACCACGTCATGAC. *TB13081* was initially identified as heterozygous segregating family. One heterozygous plant was selfed and homozygous progenies (both WT or mutant) were identified by Sanger sequencing and further selfed to produce seed for phenotypic evaluation.

Genetic mapping of short-root mutant *TM5992*

For genetic mapping of short-root mutant *TM5992*, seeds were immersed in a 0.5% sodium hypochlorite solution for 5 min, rinsed with demineralised water and incubated in the dark at 28°C for 24 h. Germinated seeds were placed between two sheets of 50 × 25 cm of filter paper (Carta filtro Labor, Gruppo Cordenons SpA, Milan, Italy) soaked in demineralised water, rolled, positioned vertically in a 5 l plastic beaker with 1 l of demineralised water and grown for 10 d at 24°C with a 16 h photoperiod. Bulked segregant analysis (BSA) (Michelmore *et al.*, 1991) was carried out using 7 d old F_2 plants derived from the cross-*TM5992* × Barke (a 2-row barley cv). For bulks preparation, 15 WTs (bulk +/+) and 15 short-root (bulk −/−) individuals were chosen. DNA from a leaf of each selected plant was extracted with a commercial kit (Macheray-Nagel Nucleospin Plant II) and bulked together in equal amounts in two (+/+ and −/−) bulks, reaching a final concentration of 50 ng μl^{-1}. The two DNA bulks along with eight short-root single-plant DNA samples and eight WT single-plant DNA samples were genotyped using the 9 k Illumina Infinium iSelect barley SNP array (Comadran *et al.*, 2012). SNPs signal was analysed with the GenomeStudio software (Illumina, San Diego, CA, USA) calculating the delta theta score as the squared difference between the theta values (Hyten *et al.*, 2008) of the two bulks.

Exome capture and sequencing

DNA samples from *TM5992* were subjected to exome capture (Mascher *et al.*, 2013b) and Next Generation Shotgun sequencing with Illumina HiSeq2000 PE100, at IPK, Gatersleben, Germany. Mutation mapping was carried out using previously described pipeline (Mascher *et al.*, 2014). Reads were aligned to the reference genome sequence of barley cultivar Morex (Mascher *et al.*, 2017) by means of the Bwa-Mem algorithm v.0.7.4 (Li & Durbin, 2009). Sorting was performed with Novosort (Novocraft Technologies SDN BHD) and read mapping statistics were obtained with Samtools (Li *et al.*, 2009; Li, 2011). Only reads uniquely mapped to the reference sequence were kept for downstream analysis. Variant calling was performed via Samtools mpileup, considering as filtering criteria a minimum call quality of Phred score ≥ 40 and a minimum coverage of 10×. At each variant position, mutant allele frequencies were calculated as the number of reads supporting the mutant allele on the total number of reads (DV/DP in the Variant Call Format file), with a custom AWK script (Mascher *et al.*, 2014). A variant was considered private to a certain mutant when it showed a mutant allele frequency not lower than 0.9. In order to remove Morex intra-cultivar standing variation, we called the mutant-identified SNPs in a barley diversity panel (267 accessions) (Russell *et al.*, 2016) and focused on the panel target region (i.e. regions showing a minimum coverage of 10× in 95% of the accessions). We further considered only variants showing a maximum mutant allele frequency of 0.1 across the panel samples. To focus on the region previously targeted by the SNP array-based BSA described above, the resulting SNP dataset was merged to the POPSEQ map (Mascher *et al.*, 2013a) to retrieve the POPSEQ positions of the sequenced BACs. Called mutations were intersected with the annotation of the barley cv Morex reference (Mascher *et al.*, 2017) and SNP effects were predicted with SNPEff (Cingolani *et al.*, 2012).

Nondestructive X-ray microCT root phenotyping of barley *PIN1a* mutants

Morex and *Hvpin1a* mutant alleles *TM5141* and *TM5992* ($n = 6$ independent replicates) were pregerminated in Petri dishes for 1 d at 21°C in dark. Equally germinated seedlings were transferred to PVC columns (8 cm diameter, 15 cm height) filled with well water sandy loam soil and grown until 9 d after germination. Each column was scanned using a Phoenix v|tome|x M® CT scanner (GE Measurement & Control Solutions, Wunstorf, Germany) at the Hounsfield Facility (University of Nottingham, Sutton Bonington Campus, UK), using a voltage and current of 180 kV and 180 µA, respectively, also at a voxel size resolution of 55 µm, with the specimen stage rotating through 360 degrees at a rotation step increment of 0.166 degrees over a period of *c.* 75 min, so a total of 2160 projection images were obtained by averaging 4 frames with an exposure of 250 ms each, at every rotation step. A 0.1 mm Copper filters was applied for the scans in front of the exit window of the X-ray tube. Scans were reconstructed into 16-bit greyscale 3D volumes using DatosRec software (GE Sensing and Inspection Technologies, Wunstorf, Germany). Reconstructed image stacks were segmented and root traits where quantified using RooTrak (Mairhofer *et al.*, 2012).

Barley root growth kinetics and root tip imaging

Root length data of barley cv Morex, *TM5992*, *TM5141*, Barke, TB_WT and *TB13081* were tracked daily for 3–5 d to assess the root growth kinetics. Only roots touching the agar surface were considered for the analysis. From the same roots, root tip samples were sectioned at 1.5 cm from the root mature zone (mid root region) and an adapted protocol from (Kurihara *et al.*, 2015; Ursache *et al.*, 2018) was used to prepare root tips for confocal imaging. Samples were fixed in paraformaldehyde for 1.5 h in

vacuum and then were left on ClearSee solution for 7 d before staining with Yellow Direct 96 dye in vacuum for 1.5 h. Cell counting from epidermal, cortical and central metaxylem tissues were performed using image stacks which have been imported in FIJI (IMAGEJ) and then aligned in order to have an in-focus image of the whole root apical meristem (RAM) which includes cells from columella to the first visible root hair.

Barley and brachypodium mutants and WT root cross sectioning

An adapted protocol from (Atkinson & Wells, 2017) was used for root cross-sectioning and confocal imaging of barley *pin1a* mutant alleles (*TM5992*, *TM5141* and *TB13081*) and brachypodium *pin1a* and *pin1b* mutants. Root sections of *c.* 1.5 cm were taken from the root mature zone (mid root region) and fixed in 4.5% agarose blocks. Blocks where then sliced (Slice height = 100 µm, Frequency = 50 Hz, Amplitude = 1 mm) and for barley, the samples were stained either using calcofluor white for 30 s–1 min before confocal imaging or a combination of Calcofluor White (Sigma 18909-100ML-F) and Basic Fuchsin to stain lignin (Ursache *et al.*, 2018). For this latter method, the agarose slices obtained from the vibratome were then stained with a 50% mixture of Calcofluor White and Basic Fuchsin (0.2%) for 5 min, washed 2 times in ClearSee every 30 min and then left clearing for 2 d in a fresh ClearSee solution. Images were collected using confocal microscope Leica-SP5 by exciting root cross-sections with UV laser at 405 nm for calcofluor white and 543 nm for Basic Fuchsin. For brachypodium cross-sectioning, plants were dipped in water for 30 min–1 h before collecting the samples and fixing them in agarose blocks. This avoids roots getting hyper oxidated which causes cell wall to degrade and turn brown in colour, compromising the staining and the imaging. Samples were then stained as above using Calcofluor White for 30 s–1 min and imaged using confocal microscope Leica-SP5.

Protein structure and binding site prediction

ALPHAFOLD2 (Jumper *et al.*, 2021; Mirdita *et al.*, 2022) was used to predict the structures of the full-length HvPIN1A protein separately using the WT sequence and the two-point mutations (TM5141 and TM5992). Since these *de novo* structure predictions did not reveal any significant structural changes in the regions surrounding the sites of the point mutations compared to the WT, the WT sequence was further analysed via PHYRE2.0 (Kelley *et al.*, 2015) and SUSPECT (Yates *et al.*, 2014) webservers to study the effects of mutations on the protein structure, stability, and possible function. This analysis revealed a strong sequence conservation and mutational sensitivity at position 490 compared to position 75 in the sequence, indicating a possible effect of the mutations at these positions on protein structure stability and function. To probe this further, binding sites were predicted on the WT structure using the DOGSITESCORER (Volkamer *et al.*, 2010) algorithm and auxin was computationally docked into the predicted sites using JAMDA (Flachsenberg *et al.*, 2024).

NPA treatment

For barley, germinated seedlings of WT Morex were transferred to paper rolls supplemented with DMSO and DMSO with 1, 5, 25 and 50 µM NPA and grown for 5 d. The paper rolls were initially soaked with 30 ml of treatment solution before germinated seeds were placed on them. Once prepared, the paper rolls were placed in 500 ml cylinders containing 100 ml of solution. To maintain adequate moisture, 5 ml of solution was added to each cylinder daily. Seedlings were then grown for 5 d in a growth room under conditions of 21°C temperature, 16 h : 8 h, day : night cycle, and 125–150 µmol m^{-2} s^{-1} light intensity. Root growth images were taken and then sections of *c.* 1.5 cm were harvested from the mature root zone (mid root region) and cross-sectioning was performed as described in the method section: *Barley and brachypodium mutants and WT root cross-sectioning*.

NAA treatment

Seedlings of barley WT (Morex) and *Hvpin1a* mutants (TM5141 and TM5992) were pregerminated in darkness for 1 d before being transferred to either 1% agar mock media with DMSO or 1% agar media supplemented with 100 nM NAA and were grown for 3 d under a 16 h : 8 h, day : night cycle at 21°C. Root growth images were taken and then root sections of 1.5 cm were harvested from the mature root zone (mid root region) and cross-sectioning was performed as described in the section above. Cross-sections were stained using Basic Fuchsin and Calcofluor White using the protocol described above (see 'Barley and brachypodium mutants and WT root cross-sectioning' in the Materials and Methods section).

Results

A novel barley short-root mutant shows defects in root growth rate and meristem size

The barley mutant line *TM5992*, identified in the TILLMore TILLING population, exhibited a short-root phenotype (Fig. 1a). This phenotype was further characterised using 2D and 3D root phenotyping methods. A growth pouch-based method (Atkinson *et al.*, 2015) validated the short-root phenotype, while the noninvasive X-ray microCT imaging (Mairhofer *et al.*, 2015) directly confirmed it in soil (Figs 1b, S2).

To elucidate the cellular basis of the *TM5992* root length defect, we initially monitored the root growth rates of mutant *TM5992* and WT Morex lines grown vertically on 1% agar plates. Root growth analysis during the first 5 d postgermination revealed a significantly slower growth in *TM5992* during the initial 2 d, compared to the accelerated growth observed in the Morex. Subsequently, over the next 3 d, the growth rate decelerated in both genotypes compared to the initial 2 d. Nevertheless, *TM5992* exhibited more than twice the reduction in growth rate compared to Morex (Fig. 1c).

Next, we investigated whether these growth differences were due to altered sizes of root apical meristem and/or elongation

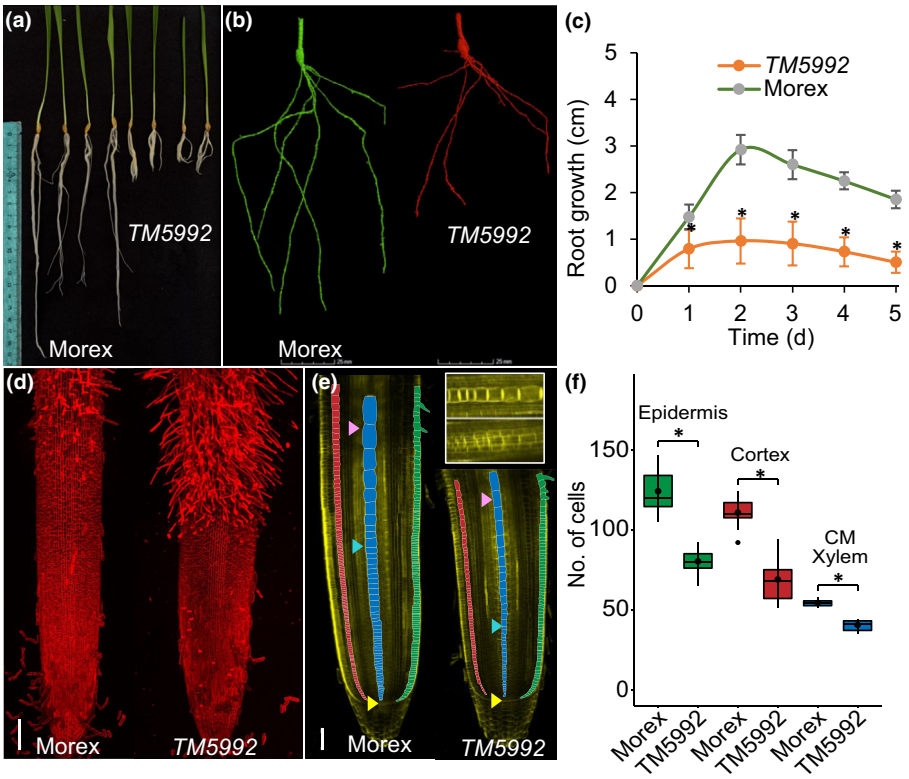

Fig. 1 Barley (*Hordeum vulgare*) mutant *TM5992* shows short-root phenotype with developmental defects. (a, b) Representative images showing root growth of *TM5992* and Morex (wild-type) in (a) paper rolls after 9 d (b) sandy loam soil filled columns after 10 d, imaged using X-ray microCT, Bar, 25 mm. Data quantification in Supporting Information Fig. S2(a,b). (c) Line graph showing root growth rate over 5 d postgermination on 1% agar plates. Mean and SD from 3 biological replicates, > 7 seedlings per replicate. *Indicates significance (*P*-value < 0.01, *t-test*). (d) Representative maximum projection confocal images of 7 d old root tips stained with Propidium Iodide showing differences in root hair differentiation zones and root hair density. Bar, 200 μm. (e) Representative confocal image of longitudinal sections of 7 d old root tips stained with Yellow Direct 96 stain showing difference in root growth zones and irregularities in vasculature. Bar, 100 μm. Green, red and blue filled cells mark epidermis, cortex and central metaxylem (CM Xylem) tissues, respectively, which were used to quantify number of cells between quiescent centre (yellow arrowhead) and first visible root hair (magenta arrowhead; differentiation zone). Turquoise arrowhead marks the first elongating metaxylem cell (highlighting elongation zone). The white bordered inset box indicates the irregularities in the CM Xylem tissue (brighter stained cells) of *TM5992* (lower panel) compared to Morex (upper panel). (f) Box plot showing number of cells in root epidermis, cortex and xylem tissues between quiescent centre and first visible root hair (as shown in images in e). > 7 seedlings per genotype used. *Indicates significance (*P*-value < 0.01, *t-test*). Dots and horizontal lines inside the box indicates mean and median, while dots outside the box indicate outlier data points.

zones, where cells divide and expand, respectively. Root zone measurements were performed by generating maximum surface projection images of 7-d-old root tips stained with propidium Iodide, using a confocal microscope. This approach revealed that roots of mutant line *TM5992* had shorter apical meristem and elongation zones compared to the Morex, causing the root hair differentiation zone in the mutant to appear closer to the root apex (Fig. 1d).

To determine whether cell division or elongation was affected in root tissues, we cleared 7-d-old root tips using ClearSee and stained them with Yellow Direct 96 stain (Fig. 1e). This enabled us to visualise and measure barley root cell numbers and lengths in cortical, epidermal and central metaxylem tissues from the stem cell initials at the root tip to the first differentiated root hair (Fig. 1f). This validation confirmed that the number and length of cells in the meristem and elongation growth zones were significantly different in *TM5992* compared to Morex. We also observed an increased root hair density (Fig. 1d) and irregularities around the central metaxylem (Fig. 1e) in the mutant line compared to Morex, suggesting that *TM5992* has root anatomical developmental defects. Taken together, our results indicate that the short-root phenotype of *TM5992* is likely due to a slower root growth rate and developmental defects.

The short-root phenotype is caused by a recessive mutation in the *HvPIN1a* gene

To pinpoint the underlying genetic basis of the short-root phenotype in *TM5992*, we tested its inheritance by crossing *TM5992* with the 2-row barley cv Proctor. F_1 plants exhibited a WT phenotype, whereas evaluation of 91 F_2 plants for root length revealed segregation for either short or WT roots (example given in Fig. 2a). Numbers and rate of phenotypic classes fitted a Mendelian pattern (72 : 19 WT : short-root plants, P = ns. χ^2 test 3 : 1). These results revealed that the root phenotype segregating in the cross-*TM5992* × Proctor was controlled by a single locus, with a WT dominant allele from cv Proctor and a mutated recessive allele from *TM5992*.

New Phytologist

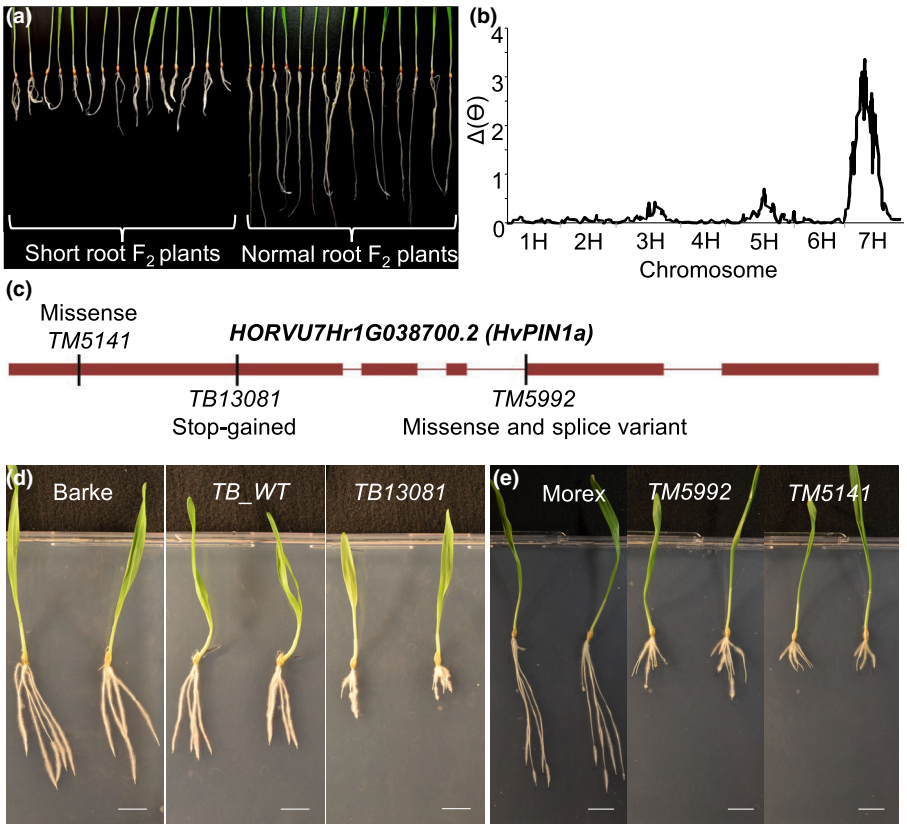

Fig. 2 Mutation in *HvPIN1a* causes a short-root phenotype and developmental defects. (a) F2 plants from the cross-*TM5992* × barley cultivar Proctor utilised in bulked DNA samples for SNP-based bulked segregant analysis (BSA). (b) Genome-wide plot of unbalanced allelic frequency from SNP-based BSA. ▵(θ) parameter represents the difference in allele frequency for each tested SNP. (c) A representation of *HvPIN1a* (gene model *HORVU7Hr1G038700.2*) with position of *TM5992* and additional mutant alleles identified from TILLMore (*TM5141*) and Barke (*TB13081*) TILLING collections. (d, e) Representative images showing short-root phenotypes of *Hvpin1a* mutant alleles and their respective background genotypes. Bar, 2 cm. TB_WT is a Barke TILLING background containing all mutations except *Hvpin1a*. Growth rate data quantification in Supporting Information Fig. S3.

A SNP-based BSA was performed to genetically map *TM5992* using the F_2 population. BSA results indicated that the mutated locus mapped on chromosome 7 (Fig. 2b), in a large pericentromeric region spanning *c* 200 Mb between markers *SCRI_RS_150016* and *BOPA1_4850–969* (38.8–68.4 cM based on the barley POPSEQ reference map) (Beier *et al.*, 2017). To pinpoint the mutation, we conducted exome sequencing of *TM5992* and mapped the reads to the Morex reference genome. A total 27 missense variants were identified to be in the coding sequences genome-wide (Dataset S1). All mutations were G>A transitions, as expected based on NaN_3 chemical treatment (Talamè *et al.*, 2008). However, within the chromosome 7H region highlighted by BSA only three coding genes were found to carry mutations in *TM5992* compared to Morex. These genes were *HORVU7Hr1G029650* at 47.78 cM, annotated as SEUSS transcriptional co-repressor; *HORVU7Hr1G038520* at 64.36 cM, annotated as Nuclear Migration protein and *HORVU7Hr1G038700* at 64.75 cM, annotated as auxin efflux carrier family protein (*HvPin1a*).

To validate which mutation in these three candidate genes conferred the short-root defect, we investigated alleles isolated from a different mutant population (background of cv Barke) (Gottwald *et al.*, 2009). We identified line *TB13081*, carrying a heterozygous premature stop codon mutation in the first exon of *HvPin1a* (Fig. 2c). Seedlings homozygous for this mutation showed a clear short-root phenotype compared to TB_WT, a Barke TILLING background containing all mutations except *HvPin1a* (Fig. 2d). Subsequently, a third *HvPin1a* mutant allele (*TM5141*) was found within the TILLMore population, which lacked any mutation within *HORVU7Hr1G029650* and *HORVU7Hr1G038520* (two other genes identified in BSA that had mutations in *TM5992*). Line *TM5141* harbours a missense mutation within the first exon and showed an even stronger short-root phenotype compared to *TM5992* (Fig. 2c,e). Analyses of root growth rate and root development in *TM5141* and *TB13081* revealed results highly similar to those observed in *TM5992* (Figs S3, S4).

While the mutation in *TB13081* (Y231*) introduces a premature stop codon, those in *TM5992* (G490E) and *TM5141* (D75N) lead to missense substitutions. To elucidate how these substitutions disrupt gene function, we mapped them onto the predicted HvPIN1a protein structure using AlphaFold2 (Jumper *et al.*, 2021). Overall, the predicted WT and mutant protein structures displayed remarkable similarity in regions containing the mutations (Fig. S5a,d). However, G490 is a highly conserved residue sensitive to mutation (Fig. S5c) and resides close to a predicted binding pocket on the WT protein structure (Fig. S5d). Therefore, in *TM5992*, the G490E substitution, replacing a neutral glycine with a negatively charged glutamic acid, is highly likely to alter the electrostatic properties of this pocket and consequently impact PIN1A function in this region. Residue D75 has a low sequence conservation but moderate sensitivity to mutation (Fig. S5b). Thus, in *TM5141*, the D75N substitution, changing a negatively charged aspartate to positively charged asparagine, is also likely to affect the local structural stability of PIN1A. To probe this further, we predicted potential binding sites on the WT structure and

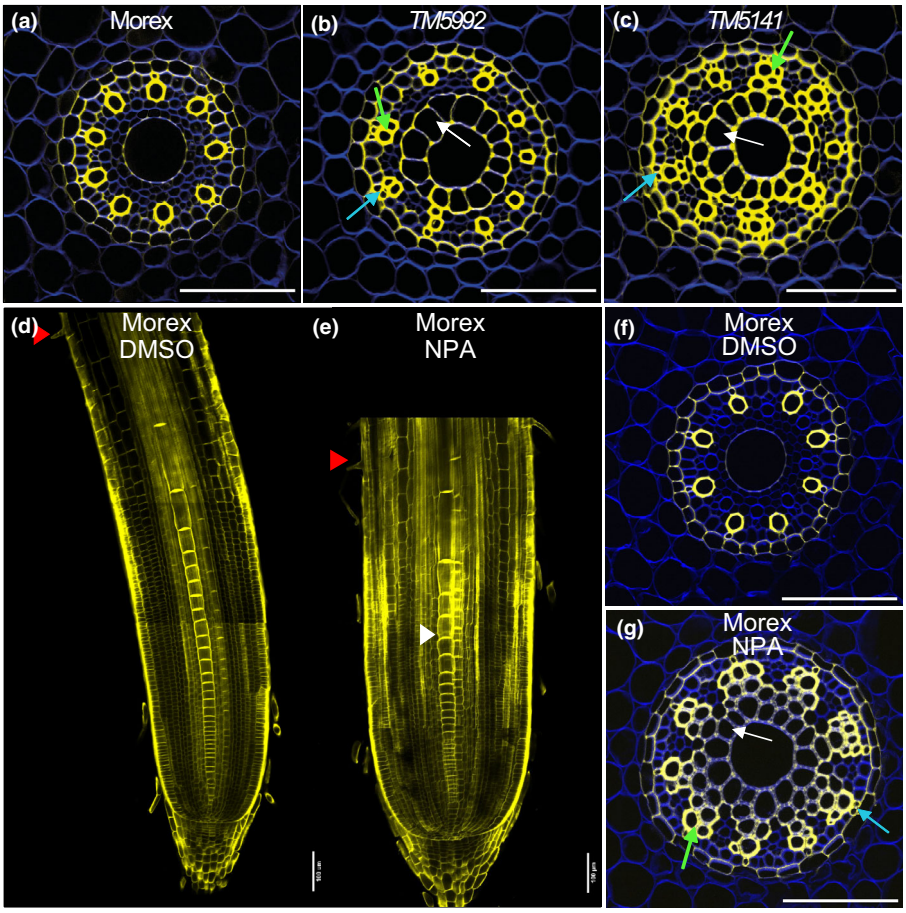

Fig. 3 Barley (*Hordeum vulgare*) *pin1a* mutant alleles show root vascular defects that can be mimicked by blocking PIN activity in Morex by NPA treatment. (a–c) Representative images showing root cross-section of Morex (a) and *Hvpin1a* mutant alleles *TM5992* (b) and *TM5141* (c). Seedlings were grown vertically for 4 d on 1% agar and mid regions (*c*. 3–4 cm from the root apex) of the seminal root were cross-sectioned using vibratome, stained with a 50% mixture of Calcofluor White and Basic Fuchsin (see Materials and Methods section) and imaged using confocal microscope. Blue, green and white arrows indicate irregularities in protoxylem, peripheral metaxylem vessels and first inner parenchymatic cell layer around the central metaxylem. Bar, 100 μm. $n > 3$ independent biological replicates and $n > 6$ seedlings per replicate. (d–g) Representative images showing Yellow Direct 96 stained longitudinal sections (d, e) and 50% mixture of Calcofluor White and Basic Fuchsin stained root cross-sections (f, g) of 5-d-old seedlings of Morex, grown on 1% agar supplemented with DMSO (control) and 50 μM NPA dissolved in DMSO. Bar, 100 μm (d, e) and 50 μm (f, g). Red arrowhead (d, e) indicates the first visible root hair and white arrowhead shows visible defects in vascular patterning. Blue, green and white arrows in (g) indicate irregularities in protoxylem, peripheral metaxylem vessels and first inner parenchymatic cell layer around the central metaxylem. $n = 3$ independent biological replicates, and seminal roots from $n > 6$ seedlings were analysed per replicate.

computationally docked auxin into the predicted sites. Two high-ranking binding sites with favourable auxin docking scores were predicted close to the sites of both these mutations (Fig. S5d), indicating that either of the G490E or D75N substitutions are likely to have a strong negative effect on auxin binding in these regions and hinder overall protein function.

Taken together, the results of root growth and the analysis of mutations on PIN1a protein structure function provide conclusive evidence that mutated *HvPin1a* is likely responsible for the short-root phenotype observed in *TM5992*, *TM5141* and *TB13081*.

HvPIN1a is essential for vascular patterning in barley roots

Longitudinal sections revealed striking irregularities in the root vasculature of all three *Hvpin1a* mutant alleles compared to their respective WT backgrounds (Figs 1e, S4a,b). To further investigate these irregularities, we examined cross-sections of 7-d-old mutant alleles and WT root samples grown in 1% agar plates (Figs 3a–c, S6). Remarkably, all mutant alleles showed enlarged cells in the Inner Parenchymatic Cell Layer (IPSL) adjacent to the central metaxylem, with a correspondingly smaller number of cells in that cell layer compared to their WTs (Fig. S7). This cell layer enlargement was associated with a significantly larger stele diameter in all mutant alleles compared to their WTs (mean increase > 13% in *TM5992* and *TM5141* compared to Morex and > 20% bigger in *TB13081* compared to Barke and TB_WT) (Fig. S8). Consequently, the root tips of all mutant alleles were slightly thicker than their WT controls (Fig. S8c,d).

Basic Fuchsin staining of *Hvpin1a* mutant allele root cross-sections showed increased staining intensity in the central metaxylem, its adjacent inner parenchymatic cell layer, and the

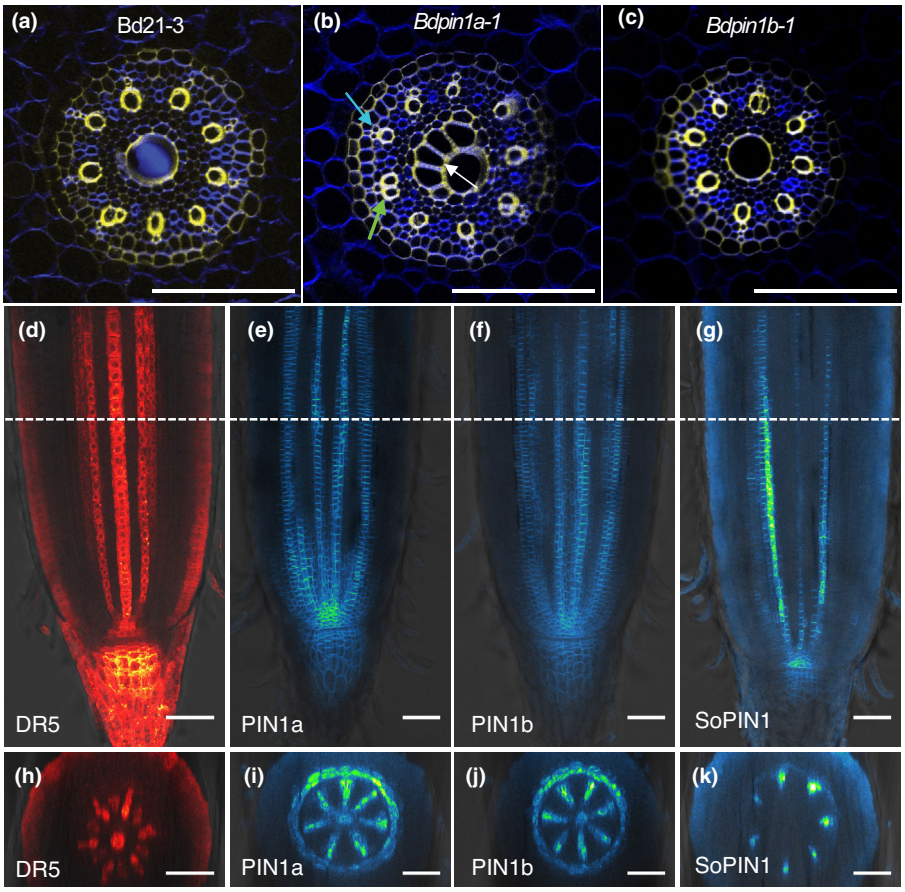

Fig. 4 The role of PIN1a in root vascular patterning is conserved in cereal model brachypodium (*Brachypodium distachyon*). (a–c) Representative confocal images of root cross-sections of wild-type brachypodium accession Bd21-3 (a), *Bdpin1a* (b) and *Bdpin1-b* (c) mutants. Seedlings were vertically grown for 7 d on 1% agar and mid regions (*c*. 2–3 cm from the root apex) of the main root were cross-sectioned, stained with 50% mixture of calcofluor white and Basic Fuchsin, and imaged using confocal microscope. $n > 3$ independent biological replicates and $n > 5$ seedlings per replicate were analysed. Bar, 100um. Blue, green and white arrows in (b) indicate irregularities in protoxylem, peripheral metaxylem vessels and first parenchymatic cell layer around the central metaxylem. (d–k) Representative confocal images showing brachypodium roots expressing (d) auxin response reporter DR5, (e, f) auxin efflux carrier reporters PIN1a, PIN1b and SoPIN1 reporters (O'Connor *et al*., 2017). Bar, 100 μm. (h–k) represents orthogonal views of (d–g, respectively) showing *YZ* axis (cross-sections) in root meristem at position marked by the white dotted line. Bar, 100 μm.

neighbouring cells of peripheral metaxylem and protoxylem, compared to the WT. These signals suggest enhanced lignification of secondary cell wall and possibly ectopic divisions in these tissue types (Fig. 3a–c). Further image quantification confirmed that among *Hvpin1a* mutants in Morex background, *TM5141* displayed the greatest deposition of lignin in the stele and more pronounced short-root phenotype compared to *TM5992* (Fig. 2e). Overall, the increased numbers of lignified cells indicated that *HvPIN1a* could be important for patterning or differentiation of root vascular tissues.

To directly validate the role of polar auxin transport (PAT) in controlling the root vascular patterning in barley, we employed the PAT inhibitor NPA. We investigated its impact on root growth and anatomy by treating Morex seedlings on agar containing increasing NPA concentrations (1, 5, 25 and 50 μM). At 5–50 μM NPA, roots phenocopied the short-root phenotype of *Hvpin1a* mutant alleles (Figs 3d,e, S9). Consistent with this, longitudinal and cross-section analysis revealed similar developmental and anatomical defects in NPA-treated WT Morex roots compared to the mutants (Figs 3f,g, S10). These findings demonstrate that blocking PIN activity with NPA mimics the short-root and vascular developmental defects observed in *Hvpin1a* mutants, strongly supporting the crucial role of HvPIN1a in PAT and root vascular patterning in barley. Additionally, the exogenous application of 100 nM NAA could not restore the WT phenotypes in *Hvpin1a* mutants (Fig. S11), suggesting that elevating auxin levels alone is not sufficient, rather, functional PIN1a is required to distribute the auxin correctly in relevant tissues.

PIN1a plays a conserved role regulating root vascular patterning in other cereals

HvPIN1a belongs to a clade of three *PIN1*-related genes in the barley genome (Fig. S1). Phylogenetic analysis revealed that barley PIN1 members exhibit a high degree of conservation with brachypodium PIN1 family members (Fig. S1). We initially investigated whether the function of *HvPIN1a* in root growth and root vascular patterning was conserved in brachypodium by characterising the root length and root anatomy of a recently described *Bdpin1a* mutant line (O'Connor *et al*., 2014, 2017). *Bdpin1a* mutant showed shorter primary root compared to the WT (*Brachypodium distachyon* accession 21.3) Bd21.3 roots (Fig. S12a,b), but not as striking as observed for *Hvpin1a* mutant alleles (Fig. 2d,e). Further, root cross-section analysis revealed that *Bdpin1a* roots had similar defects as *Hvpin1a* mutants such as irregular central metaxylem, larger parenchymatic cells surrounding central metaxylem vessel and decreased number of cells in this surrounding layer (Figs 4a,b, S12c–f) but had smaller stele diameter, contrary to observed for *Hvpin1a* mutants. Hence, *BdPIN1a* and *HvPIN1a* appear to play some orthologous developmental functions.

As the PIN1a and PIN1b duplication in grasses is conserved and SoPIN1 and PIN1 clades appear to mediate distinct functions (O'Connor *et al.*, 2014, 2017), we wondered whether any functional redundancy exists between PIN1a and PIN1b in controlling root growth and root vascular patterning. As no material was available to investigate the role of *HvPIN1b* in root vascular patterning, we were able to characterise anatomy in a recently described *Bdpin1b* mutant line (O'Connor *et al.*, 2014, 2017). However, we did not observe any patterning defects in *Bdpin1b* mutants (Figs 4c, S12c–f). Although we cannot conclude that PIN1b necessarily behaves the same way in brachypodium and barley, our results indicated that, while PIN1b may function redundantly with PIN1a to control vascular patterning, PIN1a plays a master regulatory role, and this is likely to be conserved across cereal species.

We noted that the *Bdpin1a* and *Hvpin1a* patterning defects are mainly associated with shape of central metaxylem and surrounding parenchymatic cell layer. To explore whether PIN1 clade members are specifically expressed in these root vascular cell types, we examined available GFP-based reporters of brachypodium PIN1a and PIN1b (and SoPIN1) for differences in their expression domains. Analysis of PIN1 reporters revealed both BdPIN1a and BdPIN1b are expressed redundantly in root vasculature tissues specifically in protoxylem and metaxylem (central and peripheral), while SoPIN1 is mainly expressed in the peripheral metaxylem vessels (Fig. 4e–g). The overlapping spatial expression patterns revealed for PIN1a and PIN1b suggest they could function redundantly to regulate vascular patterning. Nevertheless, genetic evidence demonstrates that PIN1a may play a more critical regulatory role patterning vascular tissues in cereal roots.

Discussion

Studies across different monocot species, including the cereal model brachypodium (O'Connor *et al.*, 2014, 2017) and maize (Forestan *et al.*, 2012), have highlighted the impact of genome duplication events in monocots on PIN family members. This duplication has led to an expansion of the PIN family compared to the eudicot model Arabidopsis, suggesting a high level of sub-functionalisation among monocot PIN members. PIN1 members, such as AtPIN1 and BdPIN1, have previously been shown to play key roles in leaf vascular patterning (Gälweiler *et al.*, 1998; Scarpella *et al.*, 2006; O'Connor *et al.*, 2014). In Arabidopsis, PIN1 is a key regulator of polar auxin transport and is expressed in differentiating cell lineages of developing root vascular tissues including xylem precursors that is protoxylem and metaxylem (Omelyanchuk *et al.*, 2016). In brachypodium, PIN1 is functionally diversified and has two duplicated PIN1 members, PIN1a and PIN1b, and a phylogenetically sister to the PIN1 clade, SoPIN1. Together, they recapitulate expression domains and polarisation behaviours observed for AtPIN1 in Arabidopsis (O'Connor *et al.*, 2014, 2017). Among cereals, PIN1 members have been shown to have different expression patterns. For instance, ZmPIN1a and ZmPIN1b are broadly expressed across different organs and tissues in maize (Forestan *et al.*, 2012), whereas in brachypodium, BdPIN1a and BdPIN1b are expressed primarily in the inner tissues of the apical shoot primordia (O'Connor *et al.*, 2014). This suggests further levels of sub-functionalisation of PIN1 members within cereals. AtPIN1 is expressed in roots and its mutants display a low penetrance phenotype with either ectopic or loss of protoxylem differentiation (Bishopp *et al.*, 2011). While previous studies in maize (Forestan *et al.*, 2012) and rice (Li *et al.*, 2019, 2022) showed expression of PIN1 members in root apex and their role in root growth regulation, it remained unclear whether these cereal PIN1 members exhibit any root vascular phenotypes.

This paper reports the characterisation a barley mutation in the *HvPIN1a* auxin efflux carrier encoding gene which causes a short-root phenotype with slower root growth rate and reduced meristem size (Figs 1, 2d,e). Closer examination of root anatomy in *Hvpin1a* mutant alleles revealed a striking vascular patterning defect. These defects included irregular central metaxylem, larger and thicker parenchymatic cells around central metaxylem vessels, higher lignification of cell walls in stele tissues including protoxylem and metaxylem (central as well as peripheral) vessels. Characterisation of a mutant line disrupting the orthologous *BdPIN1a* gene in brachypodium revealed a similar root vascular patterning defect. These results for the first time show that PIN1a plays a key role regulating root vascular patterning in cereals. Moreover, we show that when treated with high concentrations of NPA, barley WT seedlings display root anatomical defects resembling those of *Hvpin1a* mutant alleles.

Puzzlingly, *BdPIN1a* and its closely related homologue *BdPIN1b* exhibit overlapping expression patterns in brachypodium root vascular cell types. Using DR5 and BdPIN1a, BdPIN1b and SoPIN1 reporters revealed that such gene expression accumulates surrounding the areas where auxin accumulates in the vasculature tissues. Specifically, BdPIN1a and BdPIN1b expression is localised in the central metaxylem and peripheral metaxylems (as well as the endodermis), while SoPIN1 expression is localised in only the peripheral metaxylem region. Interestingly, we only observed a vasculature patterning defect in *Bdpin1a* but not in *Bdpin1b* mutant roots. This observation contrasts results in *Bdpin1b* leaves which reveals BdPIN1b plays a more important vascular patterning role in this organ (Leyser, 2005; Xi *et al.*, 2016). Accordingly, a moderate root length reduction was observed in *Bdpin1b* compared *Bdpin1a* mutants where a more evident reduction was observed in the shoot length in these mutants when compared to WT (Fig. S12a). Our mutant studies suggest that members of the PIN1 clade in cereals have undergone a process of sub-functionalisation, resembling the process seen in brachypodium during shoot organogenesis. However, in contrast to what happens in the shoot (O'Connor *et al.*, 2014, 2017), we hypothesise that BdPIN1a and BdPIN1b synergically regulate auxin flux in the root vasculature, rather than being in between vasculature and epidermal tissues, where BdPIN1a plays a prevalent role. In addition, our study clearly demonstrates that also in other cereals such as barley, conserved members of the PIN1 clade, such as PIN1a, play a key role regulating root growth vascular patterning in roots. However, the

crosstalk between different PIN1 members process still remains unclear due to the current unavailability of PIN1b and SoPIN1 mutants/reporters and the current challenges in developing stable DII/DR5 auxin reporters in cereals (Kirschner *et al.*, 2018). Further research is necessary to address these challenges and generate genetic resources for other barley PIN1 members. The availability of these resources will not only enable us to unravel the functional diversification of PIN1 members but also shed light on potential diversification of their interacting proteins or downstream effectors.

What is the physiological relevance of PIN1a mediated root vascular patterning in crops? Root vasculature is required for long-distance transport of water, mineral salts and molecular signalling from root to shoot. Especially metaxylem vessel organisation (number and area) is considered important for drought tolerance as it regulates hydraulic conductivity and conservative water usage (Comas *et al.*, 2013). Our results suggest that PIN1a is crucial for auxin mediated normal development of central metaxylem and its surrounding parenchymatic layer and overall root growth. Thus, PIN1a function could be important for root system architecture and conferring tolerance to drought and other abiotic stresses. Consistently, a recent study in maize demonstrated that overexpression of *ZmPIN1a* increases auxin levels in root and produces deeper root architecture system, resulting in more stress resilient plants with an increased yield under drought and phosphate starvation (Li *et al.*, 2018). Further work will be required to investigate physiological impact of observed vasculature defect in *pin1a* mutants in barley and brachypodium for water uptake in order to provide more insight for developing stress resilient crops.

Acknowledgements

We acknowledge the technical support of Simona Corneti, Anne Fiebig, Sandra Stefanelli. RF acknowledges the Hounsfield Facility Center at the University of Nottingham for all the support provided for this work. The Hounsfield Facility received funding from European Research Council (Futureroots Project, Grant agreement ID: 294729), Biotechnology and Biological Sciences Research Council of the United Kingdom and The Wolfson Foundation. HL was supported by a joint University of Adelaide – University of Nottingham PhD scholarship. This manuscript has been authored in part by LMY at UT-Battelle, LLC, under contract DE-AC05-00OR22725 with the US Department of Energy (DOE). The publisher acknowledges the US government licence to provide public access under the DOE Public Access Plan (http://energy.gov/downloads/doe-public-access-plan). R. Bhosale acknowledges support from BBSRC Discovery Fellowship (BB/S011102/1), BBSRC New Investigator grant (BB/X014843/1), and BBSRC-funded Delivering Sustainable Wheat (DSW) Partner Grant (BB/X018806/1).

Competing interests

None declared.

Author contributions

R Bhosale, MJB and SS designed research; RF, SGM, SR, R Bovina, CDJVT, HL, BSA, ANB, LMY, DHJ, CJS, DO'C and R Bhosale performed experiments and analysed data. NS, MM, RT and AB provided material and resources. R Bhosale, MJB and SS wrote the manuscript. All authors read and edited manuscript.

ORCID

Brian S. Atkinson https://orcid.org/0000-0001-8791-1613
Malcolm J. Bennett https://orcid.org/0000-0003-0475-390X
Rahul Bhosale https://orcid.org/0000-0001-6515-4922
Anthony Bishopp https://orcid.org/0000-0003-2962-9542
Aditi N. Borkar https://orcid.org/0000-0003-4361-6561
Cristovão De Jesus Vieira Teixeira https://orcid.org/0000-0003-3984-5513
Riccardo Fusi https://orcid.org/0000-0001-9785-0244
Dylan H. Jones https://orcid.org/0000-0001-8366-1995
Haoyu Lou https://orcid.org/0000-0001-6422-7157
Martin Mascher https://orcid.org/0000-0001-6373-6013
Devin O'Connor https://orcid.org/0000-0003-4071-8626
Serena Rosignoli https://orcid.org/0000-0002-4319-8761
Silvio Salvi https://orcid.org/0000-0002-0338-8894
Nils Stein https://orcid.org/0000-0003-3011-8731
Craig J. Sturrock https://orcid.org/0000-0002-5333-8502
Roberto Tuberosa https://orcid.org/0000-0001-9143-9569
Larry M. York https://orcid.org/0000-0002-1995-9479

Data availability

All study data are included in the main text and Supporting Information.

References

Adamowski M, Friml J. 2015. PIN-dependent auxin transport: action, regulation, and evolution. *Plant Cell* **27**: 20–32.

Atkinson JA, Wells DM. 2017. An updated protocol for high throughput plant tissue sectioning. *Frontiers in Plant Science* **8**: 1721.

Atkinson JA, Wingen LU, Griffiths M, Pound MP, Gaju O, Foulkes MJ, Le Gouis J, Griffiths S, Bennett MJ, King J *et al.* 2015. Phenotyping pipeline reveals major seedling root growth QTL in hexaploid wheat. *Journal of Experimental Botany* **66**: 2283–2292.

Beier S, Himmelbach A, Colmsee C, Zhang X-Q, Barrero RA, Zhang Q, Li L, Bayer M, Bolser D, Taudien S *et al.* 2017. Construction of a map-based reference genome sequence for barley, *Hordeum vulgare* L. *Scientific Data* **4**: 170044.

Benková E, Michniewicz M, Sauer M, Teichmann T, Seifertová D, Jürgens G, Friml J. 2003. Local, efflux-dependent auxin gradients as a common module for plant organ formation. *Cell* **115**: 591–602.

Bennett MJ, Marchant A, Green HG, May ST, Ward SP, Millner PA, Walker AR, Schulz B, Feldmann KA. 1996. Arabidopsis AUX1 gene: a permease-like regulator of root gravitropism. *Science* **273**: 948–950.

Bilsborough GD, Runions A, Barkoulas M, Jenkins HW, Hasson A, Galinha C, Laufs P, Hay A, Prusinkiewicz P, Tsiantis M. 2011. Model for the regulation of *Arabidopsis thaliana* leaf margin development. *Proceedings of the National Academy of Sciences, USA* **108**: 3424–3429.

Bishopp A, Help H, El-Showk S, Weijers D, Scheres B, Friml J, Benková E, Mähönen AP, Helariutta Y. 2011. A mutually inhibitory interaction between auxin and cytokinin specifies vascular pattern in roots. *Current Biology* **21**: 917–926.

Blilou I, Xu J, Wildwater M, Willemsen V, Paponov I, Friml J, Heidstra R, Aida M, Palme K, Scheres B. 2005. The PIN auxin efflux facilitator network controls growth and patterning in Arabidopsis roots. *Nature* **433**: 39–44.

Chmielewska B, Janiak A, Karcz J, Guzy-Wrobelska J, Forster BP, Nawrot M, Rusek A, Smyda P, Kedziorski P, Maluszynski M *et al.* 2014. Morphological, genetic and molecular characteristics of barley root hair mutants. *Journal of Applied Genetics* **55**: 433–447.

Cingolani P, Platts A, Wang LL, Coon M, Nguyen T, Wang L, Land SJ, Lu X, Ruden DM. 2012. A program for annotating and predicting the effects of single nucleotide polymorphisms, SnpEff. *Fly* **6**: 80–92.

Comadran J, Kilian B, Russell J, Ramsay L, Stein N, Ganal M, Shaw P, Bayer M, Thomas W, Marshall D *et al.* 2012. Natural variation in a homolog of Antirrhinum CENTRORADIALIS contributed to spring growth habit and environmental adaptation in cultivated barley. *Nature Genetics* **44**: 1388–1392.

Comas LH, Becker SR, Cruz VMV, Byrne PF, Dierig DA. 2013. Root traits contributing to plant productivity under drought. *Frontiers in Plant Science* **4**: 442.

Flachsenberg F, Ehrt C, Gutermuth T, Rarey M. 2024. Redocking the PDB. *Journal of Chemical Information and Modeling* **64**: 219–237.

Forestan C, Farinati S, Varotto S. 2012. The maize PIN gene family of auxin transporters. *Frontiers in Plant Science* **3**: 16.

Fusi R, Rosignoli S, Lou H, Sangiorgi G, Bovina R, Pattem JK, Borkar AN, Lombardi M, Forestan C, Milner SG *et al.* 2022. Root angle is controlled by EGT1 in cereal crops employing an antigravitropic mechanism. *Proceedings of the National Academy of Sciences, USA* **119**: e2201350119.

Gahoonia TS, Nielsen NE, Joshi PA, Jahoor A. 2001. A root hairless barley mutant for elucidating genetic of root hairs and phosphorus uptake. *Plant and Soil* **235**: 211–219.

Gälweiler L, Guan C, Müller A, Wisman E, Mendgen K, Yephremov A, Palme K. 1998. Regulation of polar auxin transport by AtPIN1 in Arabidopsis vascular tissue. *Science* **282**: 2226–2230.

Gasparis S, Przyborowski M, Kała M, Nadolska-Orczyk A. 2019. Knockout of the HvCKX1 or HvCKX3 gene in barley (*Hordeum vulgare* L.) by RNA-guided Cas9 nuclease affects the regulation of cytokinin metabolism and root morphology. *Cells* **8**: 782.

Gottwald S, Bauer P, Komatsuda T, Lundqvist U, Stein N. 2009. TILLING in the two-rowed barley cultivar 'Barke' reveals preferred sites of functional diversity in the gene HvHox1. *BMC Research Notes* **2**: 258.

Guenot B, Bayer E, Kierzkowski D, Smith RS, Mandel T, Žádníková P, Benková E, Kuhlemeier C. 2012. Pin1-independent leaf initiation in Arabidopsis. *Plant Physiology* **159**: 1501–1510.

Hay A, Barkoulas M, Tsiantis M. 2006. ASYMMETRIC LEAVES1 and auxin activities converge to repress BREVIPEDICELLUS expression and promote leaf development in Arabidopsis. *Development* **133**: 3955–3961.

Hyten DL, Song Q, Choi I-Y, Yoon M-S, Specht JE, Matukumalli LK, Nelson RL, Shoemaker RC, Young ND, Cregan PB. 2008. High-throughput genotyping with the GoldenGate assay in the complex genome of soybean. *Theoretical and Applied Genetics* **116**: 945–952.

Jumper J, Evans R, Pritzel A, Green T, Figurnov M, Ronneberger O, Tunyasuvunakool K, Bates R, Žídek A, Potapenko A *et al.* 2021. Highly accurate protein structure prediction with AlphaFold. *Nature* **596**: 583–589.

Kelley LA, Mezulis S, Yates CM, Wass MN, Sternberg MJE. 2015. The Phyre2 web portal for protein modeling, prediction and analysis. *Nature Protocols* **10**: 845–858.

Kirschner GK, Hochholdinger F, Salvi S, Bennett MJ, Huang G, Bhosale RA. 2024. Genetic regulation of the root angle in cereals. *Trends in Plant Science*, in press. doi: 10.1016/j.tplants.2024.01.008.

Kirschner GK, Rosignoli S, Guo L, Vardanega I, Imani J, Altmüller J, Milner SG, Balzano R, Nagel KA, Pflugfelder D *et al.* 2021. ENHANCED GRAVITROPISM 2 encodes a STERILE ALPHA MOTIF–containing protein that controls root growth angle in barley and wheat. *Proceedings of the National Academy of Sciences, USA* **118**: e2101526118.

Kirschner GK, Stahl Y, Imani J, Korff M v, Simon R. 2018. Fluorescent reporter lines for auxin and cytokinin signalling in barley (Hordeum vulgare). *PLoS ONE* **13**: e0196086.

Kurihara D, Mizuta Y, Sato Y, Higashiyama T. 2015. ClearSee: a rapid optical clearing reagent for whole-plant fluorescence imaging. *Development* **142**: 4168–4179.

Leyser O. 2005. Auxin distribution and plant pattern formation: how many angels can dance on the point of PIN? *Cell* **121**: 819–822.

Li H. 2011. A statistical framework for SNP calling, mutation discovery, association mapping and population genetical parameter estimation from sequencing data. *Bioinformatics* **27**: 2987–2993.

Li H, Durbin R. 2009. Fast and accurate short read alignment with Burrows–Wheeler transform. *Bioinformatics* **25**: 1754–1760.

Li H, Handsaker B, Wysoker A, Fennell T, Ruan J, Homer N, Marth G, Abecasis G, Durbin R, Subgroup 1000 Genome Project Data Processing. 2009. The sequence alignment/map format and SAMtools. *Bioinformatics* **25**: 2078–2079.

Li Y, Wu L, Ren M, Zhu J, Xu J, Hu H, Quan X, Huang C, Mao C. 2022. Functional redundancy of OsPIN1 paralogous genes in regulating plant growth and development in rice. *Plant Signaling & Behavior* **17**: 2065432.

Li Y, Zhu J, Wu L, Shao Y, Wu Y, Mao C. 2019. Functional divergence of PIN1 paralogous genes in rice. *Plant and Cell Physiology* **60**: 2720–2732.

Li Z, Zhang X, Zhao Y, Li Y, Zhang G, Peng Z, Zhang J. 2018. Enhancing auxin accumulation in maize root tips improves root growth and dwarfs plant height. *Plant Biotechnology Journal* **16**: 86–99.

Mairhofer S, Sturrock CJ, Bennett MJ, Mooney SJ, Pridmore TP. 2015. Extracting multiple interacting root systems using X-ray microcomputed tomography. *The Plant Journal* **84**: 1034–1043.

Mairhofer S, Zappala S, Tracy SR, Sturrock C, Bennett M, Mooney SJ, Pridmore T. 2012. RooTrak: automated recovery of three-dimensional plant root architecture in soil from X-ray microcomputed tomography images using visual tracking. *Plant Physiology* **158**: 561–569.

Mascher M, Gundlach H, Himmelbach A, Beier S, Twardziok SO, Wicker T, Radchuk V, Dockter C, Hedley PE, Russell J *et al.* 2017. A chromosome conformation capture ordered sequence of the barley genome. *Nature* **544**: 427–433.

Mascher M, Jost M, Kuon J-E, Himmelbach A, Aßfalg A, Beier S, Scholz U, Graner A, Stein N. 2014. Mapping-by-sequencing accelerates forward genetics in barley. *Genome Biology* **15**: R78.

Mascher M, Muehlbauer GJ, Rokhsar DS, Chapman J, Schmutz J, Barry K, Muñoz-Amatriaín M, Close TJ, Wise RP, Schulman AH *et al.* 2013a. Anchoring and ordering NGS contig assemblies by population sequencing (POPSEQ). *The Plant Journal* **76**: 718–727.

Mascher M, Richmond TA, Gerhardt DJ, Himmelbach A, Clissold L, Sampath D, Ayling S, Steuernagel B, Pfeifer M, D'Ascenzo M *et al.* 2013b. Barley whole exome capture: a tool for genomic research in the genus Hordeum and beyond. *The Plant Journal* **76**: 494–505.

McCallum CM, Comai L, Greene EA, Henikoff S. 2000. Targeted screening for induced mutations. *Nature Biotechnology* **18**: 455–457.

Michelmore RW, Paran I, Kesseli RV. 1991. Identification of markers linked to disease-resistance genes by bulked segregant analysis: a rapid method to detect markers in specific genomic regions by using segregating populations. *Proceedings of the National Academy of Sciences, USA* **88**: 9828–9832.

Mirdita M, Schütze K, Moriwaki Y, Heo L, Ovchinnikov S, Steinegger M. 2022. ColabFold: making protein folding accessible to all. *Nature Methods* **19**: 679–682.

Nice LM, Steffenson BJ, Brown-Guedira GL, Akhunov ED, Liu C, Kono TJY, Morrell PL, Blake TK, Horsley RD, Smith KP *et al.* 2016. Development and genetic characterization of an advanced backcross-nested association mapping (AB-NAM) population of wild × cultivated barley. *Genetics* **203**: 1453–1467.

O'Connor DL, Elton S, Ticchiarelli F, Hsia MM, Vogel JP, Leyser O. 2017. Cross-species functional diversity within the PIN auxin efflux protein family. *eLife* **6**: e31804.

O'Connor DL, Runions A, Sluis A, Bragg J, Vogel JP, Prusinkiewicz P, Hake S. 2014. A division in PIN-mediated auxin patterning during organ initiation in grasses. *PLoS Computational Biology* **10**: e1003447.

Omelyanchuk NA, Kovrizhnykh VV, Oshchepkova EA, Pasternak T, Palme K, Mironova VV. 2016. A detailed expression map of the PIN1 auxin transporter in *Arabidopsis thaliana* root. *BMC Plant Biology* **16**: 5.

Petrášek J, Mravec J, Bouchard R, Blakeslee JJ, Abas M, Seifertová D, Wiśniewska J, Tadele Z, Kubeš M, Čovanová M *et al.* 2006. PIN proteins perform a rate-limiting function in cellular auxin efflux. *Science* **312**: 914–918.

Reinhardt D, Pesce E-R, Stieger P, Mandel T, Baltensperger K, Bennett M, Traas J, Friml J, Kuhlemeier C. 2003. Regulation of phyllotaxis by polar auxin transport. *Nature* **426**: 255–260.

Russell J, Mascher M, Dawson IK, Kyriakidis S, Calixto C, Freund F, Bayer M, Milne I, Marshall-Griffiths T, Heinen S *et al.* 2016. Exome sequencing of geographically diverse barley landraces and wild relatives gives insights into environmental adaptation. *Nature Genetics* **48**: 1024–1030.

Scarpella E, Marcos D, Friml J, Berleth T. 2006. Control of leaf vascular patterning by polar auxin transport. *Genes & Development* **20**: 1015–1027.

Schreiber M, Barakate A, Uzrek N, Macaulay M, Sourdille A, Morris J, Hedley PE, Ramsay L, Waugh R. 2019. A highly mutagenised barley (cv. Golden Promise) TILLING population coupled with strategies for screening-by-sequencing. *Plant Methods* **15**: 99.

Swarup R, Bhosale R. 2019. Developmental roles of AUX1/LAX auxin influx carriers in plants. *Frontiers in Plant Science* **10**: 1306.

Swarup R, Péret B. 2012. AUX/LAX family of auxin influx carriers—an overview. *Frontiers in Plant Science* **3**: 225.

Talamè V, Bovina R, Sanguineti MC, Tuberosa R, Lundqvist U, Salvi S. 2008. TILLMore, a resource for the discovery of chemically induced mutants in barley. *Plant Biotechnology Journal* **6**: 477–485.

Ursache R, Andersen TG, Marhavý P, Geldner N. 2018. A protocol for combining fluorescent proteins with histological stains for diverse cell wall components. *The Plant Journal* **93**: 399–412.

Volkamer A, Griewel A, Grombacher T, Rarey M. 2010. Analyzing the topology of active sites: on the prediction of pockets and subpockets. *Journal of Chemical Information and Modeling* **50**: 2041–2052.

Wiśniewska J, Xu J, Seifertová D, Brewer PB, Růžička K, Blilou I, Rouquié D, Benková E, Scheres B, Friml J. 2006. Polar PIN localization directs auxin flow in plants. *Science* **312**: 883.

Xi W, Gong X, Yang Q, Yu H, Liou Y-C. 2016. Pin1At regulates PIN1 polar localization and root gravitropism. *Nature Communications* **7**: 10430.

Yates CM, Filippis I, Kelley LA, Sternberg MJE. 2014. SuSPect: enhanced prediction of single amino acid variant (SAV) phenotype using network features. *Journal of Molecular Biology* **426**: 2692–2701.

Zhang Y, Xiao G, Wang X, Zhang X, Friml J. 2019. Evolution of fast root gravitropism in seed plants. *Nature Communications* **10**: 3480.

Supporting Information

Additional Supporting Information may be found online in the Supporting Information section at the end of the article.

Dataset S1 Exome sequencing and mapping of *TM5992* reads to Morex reference identified 16 mutations within genes on Chromosome 7H. Red highlighted rows indicate three mutations within region of interest identified by Bulk Segregant Analysis.

Fig. S1 Phylogenetic analysis of PIN Protein sequences in Arabidopsis, barley, wheat, rice, maize and brachypodium.

Fig. S2 Measured root growth parameters of *TM5992* and Morex.

Fig. S3 *HvPIN1a* allelic mutant lines *TM5141* and *TB13081* exhibit similar root growth rate as line *TM5992*.

Fig. S4 *HvPIN1a* allelic mutant lines *TM5141* and *TB13081* exhibit similar root developmental defects as line *TM5992*.

Fig. S5 Structure prediction of HvPIN1a and mutation mapping.

Fig. S6 *HvPIN1a* allelic mutant line *TB13081* exhibit similar root anatomical defects as line *TM5992* and *TM5141*.

Fig. S7 *HvPIN1a* allelic mutants show enlarged parenchymatic cells in the inner stele layer surrounding central metaxylem.

Fig. S8 *HvPIN1a* allelic mutants show enlarged stele and root diameter.

Fig. S9 NPA treatment induces short-root phenotype and vascular patterning defects in the wild-type (WT) Morex roots similar to those observed in *HvPIN1a* mutant alleles.

Fig. S10 NPA treatment increases root and stele diameter in wild-type (WT) Morex similar to those observed in *HvPIN1a* mutant alleles.

Fig. S11 NAA treatment does not rescue wild-type (WT) phenotypes in *HvPIN1a* mutant alleles.

Fig. S12 Root growth and anatomy comparison between brachypodium wild-type (WT) (Bd21-3) and *Bdpin1* mutants (*Bdpin1a*, *Bdpin1b*).

Please note: Wiley is not responsible for the content or functionality of any Supporting Information supplied by the authors. Any queries (other than missing material) should be directed to the *New Phytologist* Central Office.